EUMETSAT Satellite Application Facility on Climate Monitoring

The EUMETSAT Network of Satellite Application Facilities

CM SAF
Climate Monitoring

Product User Manual

SEVIRI dataset cloud products

Edition 1

DOI: 10.5676/EUMETSAT_SAF_CM/CLAAS/V001

Fractional Cloud Cover	**CM-06**
Joint Cloud property histogram	**CM-12**
Cloud Top level	**CM-18**
Cloud Optical Thickness	**CM-35**
Cloud Phase	**CM-39**
Liquid Water Path	**CM-44**
Ice Water Path	**CM-46**

Reference Number:	SAF/CM/DWD/PUM/SEV/CLD
Issue/Revision Index:	1.2
Date:	16.10.2013

Document Signature Table

	Name	Function	Signature	Date
Author	Anke Kniffka Jan Fokke Meirink Martin Stengel	CM SAF scientist CM SAF scientist CM SAF scientist		07/10/2012
Editor	Rainer Hollmann	Science Coordinator		18/03/2013
Approval		CM SAF Steering Group		16/04/2013
Release	Martin Werscheck	Project Manager		16/04/2013

Distribution List

Internal Distribution	
Name	**No. Copies**
DWD Archive	1
CM SAF Team	1

External Distribution		
Company	**Name**	**No. Copies**
PUBLIC		1

Document Change Record

Issue/ Revision	Date	DCN No.	Changed Pages/Paragraphs
1.0	21/11/2012	SAF/CM/DWD/PUM/SEV/CLD	First official version submitted for DRI7
1.1	18/03/2013	SAF/CM/DWD/PUM/SEV/CLD	Implementation of RIDs of DRI7-SEV; editorial changes
1.2	16/10/2013	SAF/CM/DWD/PUM/SEV/CLD	Correction of DOI-number

Applicable documents

Reference	Title	Code
AD 1	CM SAF Product Requirements Document	SAF/CM/DWD/PRD/2
AD 2	CM SAF Service Specification Document	SAF/CM/DWD/SeSp/2

Reference Documents

Reference	Title	Code
RD 1	Validation Report SEVIRI Cloud Products Edition 1	SAF/CM/DWD/VAL/SEV/CLD/1.2
RD 2	Algorithm Theoretical Basis Document SEVIRI Cloud products Edition 1	SAF/CM/DWD/ATBD/SEV/CLD/1.1
RD 3	Algorithm Theoretical Basis Document SAFNWC/MSG “Cloud mask, Cloud Type, Cloud Top Temperature, Pressure, Height”	SAF/NWC/CDOP/MFL/SCI/ATBD/01, Issue 3, Rev. 0
RD 4	Algorithm Theoretical Basis Document Cloud physical products SEVIRI	SAF/CM/KNMI/ATBD/SEV/CPP/1.2
RD 5	Algorithm Theoretical Basis Document Joint Cloud property Histograms AVHRR/SEVIRI	SAF/CM/SMHI/ATBD/JCH/1.1
RD 6	SAF NWC / MSG Output Products Format Definition	SAF-NWC-CDOP-INM-SW-ICD-3_v4.0.pdf

Table of Contents

List of Tables

1 Introduction

This CM SAF Product User Manual provides information on the CLAAS datasets (CLAAS: CMSAF CLoud property dAtaset Using SEVIRI) derived from Spinning Enhanced Visible and InfraRed Imager (SEVIRI) observations onboard the EUMETSAT METEOSAT Second Generation (MSG) satellites. The covered time period ranges from 2004 to 2011, thus includes MSG1 and MSG-2, for which the transition took place in April 2007.

This manual briefly describes the historical development of CM SAF, the CLAAS data set and the current and upcoming versioning for CLAAS products. A technical description of the data sets including information on the file format as well as on the data access is provided. Furthermore details on the implementation of the retrieval processing chain, and individual algorithm descriptions are available in the algorithm theoretical basis document [RD 2]. Basic accuracy requirements are defined in the product requirements document [AD 1]. A detailed validation of the SEVIRI based parameters is available in the validation report [RD 1].

2 The EUMETSAT SAF on Climate Monitoring (CM SAF)

The importance of climate monitoring with satellites was recognized in 2000 by EUMETSAT Member States when they amended the EUMETSAT Convention to affirm that the EUMETSAT mandate is also to “contribute to the operational monitoring of the climate and the detection of global climatic changes". Following this, EUMETSAT established within its Satellite Application Facility (SAF) network a dedicated centre, the SAF on Climate Monitoring (CM SAF, http://www.cmsaf.eu).
The consortium of CM SAF currently comprises the Deutscher Wetterdienst (DWD) as host institute, and the partners from the Royal Meteorological Institute of Belgium (RMIB), the Finnish Meteorological Institute (FMI), the Royal Meteorological Institute of the Netherlands (KNMI), the Swedish Meteorological and Hydrological Institute (SMHI), the Meteorological Service of Switzerland (MeteoSwiss), and the Meteorological Service of the United Kingdom (UK MetOffice). Since the beginning in 1999, the EUMETSAT Satellite Application Facility on Climate Monitoring (CM SAF) has developed and will continue to develop capabilities for a sustained generation and provision of Climate Data Records (CDR’s) derived from operational meteorological satellites.
In particular the generation of long-term data sets is pursued. The ultimate aim is to make the resulting data sets suitable for the analysis of climate variability and potentially the detection of climate trends. CM SAF works in close collaboration with the EUMETSAT Central Facility and liaises with other satellite operators to advance the availability, quality and usability of Fundamental Climate Data Records (FCDRs) as defined by the Global Climate Observing System (GCOS). As a major task the CM SAF utilizes FCDRs to produce records of Essential Climate Variables (ECVs) as defined by GCOS. Thematically, the focus of CM SAF is on ECVs associated with the global energy and water cycle.

Another essential task of CM SAF is to produce data sets that can serve applications related to the new Global Framework of Climate Services initiated by the WMO World Climate Conference-3 in 2009. CM SAF is supporting climate services at national meteorological and hydrological services (NMHSs) with long-term data records but also with data sets produced close to real time that can be used to prepare monthly/annual updates of the state of the climate. Both types of products together allow for a consistent description of mean values,

anomalies, variability and potential trends for the chosen ECVs. CM SAF ECV data sets also serve the improvement of climate models both at global and regional scale.
As an essential partner in the related international frameworks, in particular WMO SCOPE-CM (Sustained COordinated Processing of Environmental satellite data for Climate Monitoring), the CM SAF - together with the EUMETSAT Central Facility, assumes the role as main implementer of EUMETSAT's commitments in support to global climate monitoring. This is achieved through:

- Application of highest standards and guidelines as lined out by GCOS for the satellite data processing,
- Processing of satellite data within a true international collaboration benefiting from developments at international level and pollinating the partnership with own ideas and standards,
- Intensive validation and improvement of the CM SAF climate data records,
- Taking a major role in data set assessments performed by research organisations such as WCRP (World Climate Research Program). This role provides the CM SAF with deep contacts to research organizations that form a substantial user group for the CM SAF CDRs,
- Maintaining and providing an operational and sustained infrastructure that can serve the community within the transition of mature CDR products from the research community into operational environments.

A catalogue of all available CM SAF products is accessible via the CM SAF webpage, www.cmsaf.eu. Here, detailed information about product ordering, add-on tools, sample programs and documentation is provided.

A catalogue of available CM SAF products is available via the CM SAF webpage, http://www.cmsaf.eu/. Here, detailed information about product ordering, add-on tools, sample programs and documentation are provided.

3 Compilation of the CLAAS cloud dataset

The CLAAS data set is based on 8 years of SEVIRI measurements. SEVIRI is a passive visible and infrared imager mounted on the Meteosat Second Generation satellites 1 and 2. MSG 1 and MSG 2 are geostationary satellites which, by their rotation, support an SEVIRI imaging repeat cycle of 15 minutes. SEVIRI itself is an optical imaging radiometer with 12 spectral channels ranging from the visible (approx. 0.6 µm) to the infrared of about 13.4 µm. The respective MSGs in operational mode are centred near 0°/0° latitude/longitude, where a full earth disk image includes Europe, Africa, the Middle East and the Atlantic Ocean. For the CLAAS dataset hourly resolution was applied to balance the benefits from higher accuracy with increased processing time and data amount. The horizontal resolution of a SEVIRI image is 3 x 3 km² at nadir. CLAAS covers the time-span 2004-2011, where MSG1 measurements were processed from 01/2004 – 04/2007 and MSG 2 from 04/2007 – 12/2011. Gaps of more than 24 hours in the MSG 2 time-series were filled with MSG 1 measurements, see Figure 3-1. For the derivation of our cloud products we used the Level 1.5 SEVIRI data provided by EUMETSAT. Level 1.5 data are an extension of Level1 data which are image data that were directly transferred to the EUMETSAT's ground segment. i.e. raw data before any modification has taken place. The Level 1.5 data record comprises image data that has already undergone certain modifications by EUMETSAT: it has been corrected for all unwanted radiometric and geometric effects, has been geolocated using a standardised projection, and has been calibrated and radiance-linearised. Due to the introduction of a new radiance definition by EUMETSAT on 5. 5. 2008, we use reprocessed Level 1.5 data prior this date with the base algorithm version 0201 and the near real time version 0100 afterwards to ensure homogeneity of the time series.

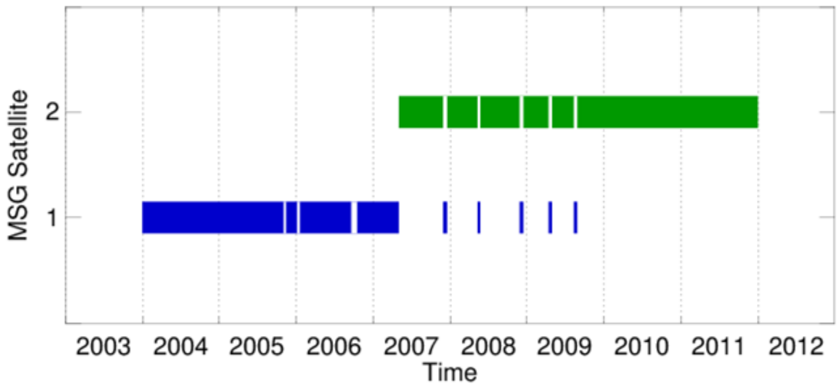

Figure 3-1: *Overview of SEVIRI measurements record at CM SAF used as basis for cloud products. Short-term data gaps are shown enlarged due to better visibility.*

The Level 1.5 radiance data record was processed with two software packages: the MSG v2010 software package by the NWCSAF (SAF to support to Nowcasting and Very Short Range Forecasting) used to derive cloud fraction and cloud top properties (Derrien and Le Gléau, 2005), and the CPP (Cloud Physical Properties) algorithm (Roebeling et al. 2006), which retrieves cloud thermodynamic phase, cloud optical thickness, cloud particle effective radius, and liquid/ice water path. For processing the SEVIRI data we adopted the following strategy: processing started for each day of a specific month at midnight, all days of a month were processed in parallel, up to 5 month were processed simultaneously. The first setting was necessary not only to speed up processing, but also to make temporal dependency calculation possible, the latter is needed to derive the cloud mask (Derrien and LeGleau, 2010).

The time-series of SEVIRI reflectances were carefully calibrated against MODIS, which improved especially the retrieval of microphysical parameters. For the two satellites static coefficients were derived, no temporal dependence was included for the first edition of CLAAS. Bhatt *et al*. (2010) found SEVIRI to be stable over time with a degradation of 5 – 8 ‰ over 3 years. With the calibration also homogenisation was performed because the same MODIS instrument was used for both, MSG 1 and MSG 2. The IR radiances of SEVIRI were left unchanged, relying on the on-board black-body calibration as the radiances definition as provided by EUMETSAT.

For a more detailed instrument specification and description of the calibration the reader is referred to the SEVIRI Algorithm Theoretical Baseline Document [RD 2].

4 Product definitions

The CLAAS cloud data set from SEVIRI provides seven cloud parameters. All cloud products are introduced in Table 4-1 with associated acronyms and units.

All parameters can be accessed on Level 2 basis, which means in original SEVIRI pixel size (3 x 3 km² at subsatellite point) and in hourly resolution. The products CFC, COT, CPH, IPW, LWP and COT are also available as daily and monthly composites on a regular latitude/longitude grid with a spatial resolution of 0.05° × 0.05° degrees. Additionally monthly mean diurnal cycle is provided with a temporal resolution of one hour. Please note that the Joint Cloud property Histogram and the monthly mean diurnal cycle fields are only available on a 0.25° x 0.25° grid due to the enhanced file size, also JCH is available on monthly basis only. All product features are listed in Table 4-2

Table 4-1: CLAAS product suite.

Product identifier	Acronym	Product title	Unit (*Level 2* / Level 3)
CM-06	CFC	Cloud Fractional Cover (or Cloud Amount).	*dimensionless* / %
CM-18	CTO	Cloud Top information, expressed either as Cloud Top Pressure, geometrical Cloud Top Height or Cloud Top Temperature.	*hPa, m or K* / hPa, m or K
CM-39	CPH	Cloud particle Phase category contribution.	*dimensionless* / %
CM-35	COT	Cloud optical thickness.	*dimensionless* / dimensionless

CM-44	LWP	Liquid Water Path	*kg/m²* / kg/m²
CM-46	IWP	Ice Water Path	*kg/m²* / kg/m²
CM-12	JCH	Joint Cloud property Histogram, consists of CTP and COT	*dimensionless*

Table 4-2: Product features concerning temporal averaging and additional resolution i.e. day and night separation, liquid water and ice as well as histogram representation.

	Daily mean	*Monthly mean*	*Monthly mean diurnal cycle*	*Monthly histograms*
CFC	✓ day/night	✓ day/night	✓	
CTO	✓	✓	✓	✓
COT	✓	✓	✓	✓
CPH	✓ liqu./ice	✓ liqu./ice	✓	
LWP	✓	✓	✓	✓
IWP	✓	✓	✓	✓
JCH				✓ liqu./ice

Acknowledging the different observation capabilities during night and during day and also taking into account existing diurnal variations in cloudiness, a further separation of results into daytime and night-time portions was done for CFC. Here, all observations made under twilight conditions (solar zenith angles between 80-95 degrees) have been excluded in order to avoid being affected by specific cloud detection problems occurring in the twilight zone.

The temporal coverage of the data sets ranges from January 2004 to December 2011.

For each cloud parameter, also various meta data and information about selected statistical parameter distributions in each grid point is available in addition to the main product content described above. Details on how to access this information is given in Section 6.

A complete description of the retrieval methods for each individual product is given in the Algorithm Theoretical Basis Documents [RD 3, RD 4, RD 5]. The general methods for SEVIRI calibration and calculation of Level 3 products are described in [RD 2].

In the following, each cloud product is shortly described regarding retrieval methods, information content and limitations. Validation results are also described shortly for each cloud product. A summary of all validation results can also be found at the end of this document (Section 10). More details on achieved validation results are given (e.g., more detailed information on accuracy and precision studies) in [RD 1]. At the end of each product description a short statement on recommended applications areas is also given.

4.1 Parameter Retrievals

4.1.1 Fractional cloud cover – CFC

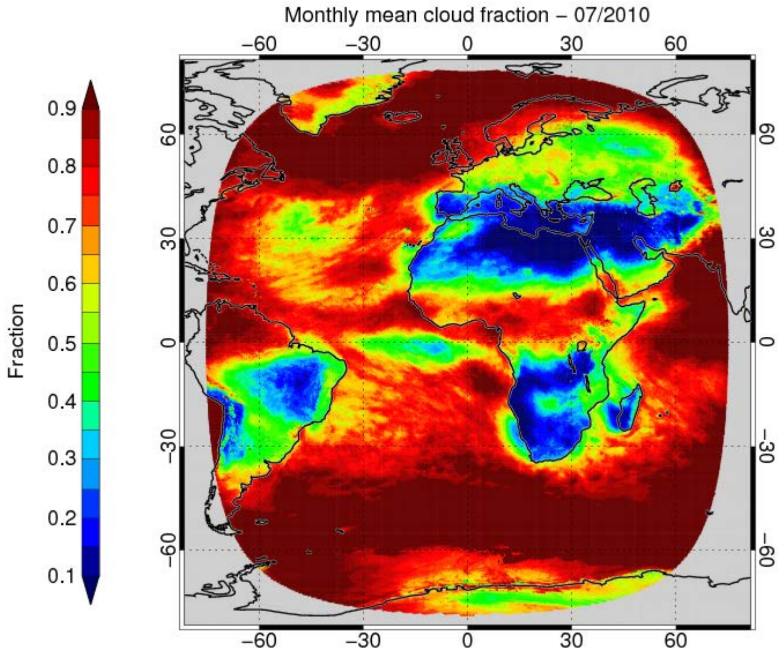

Figure 4-1: *Monthly mean of cloud fractional cover as seen by SEVIRI, July 2010.*

This product is derived directly from results of a cloud screening or cloud masking method. The cloud mask (Level 2) comprises 6 categories: Cloud filled, cloud-free, cloud contaminated and non-processed, snow/ice contaminated, undefined. The cloud fractional cover (Level 3, monthly and daily mean, as well as monthly mean diurnal cycle) is defined as the fraction of cloudy pixels per grid square compared to the total number of analysed pixels in the grid square. Pixels are counted as cloudy if they belong to the classes cloud filled or cloud contaminated. Fractional cloud cover is expressed in percent. An example, here the fractional cloud cover of July 2010, is shown in Figure 4-1.
In addition, information on the cloud type is also provided, in form of fraction per cloud type, based on all cloudy pixel. Thereby it is distinguished between the following cloud types: low, middle level, high opaque, high semi-transparent and fractional. These cloud classes are a summary of the 19 cloud classes provided by the SAF NWC msgv2010 cloud typing algorithm. Low clouds refer to types [5 - 8], middle level cloud to types [9,10], high-opaque clouds are made of types [11 - 14], while high semi-transparent clouds have types[15 - 18] and fractional clouds type 19.

Short Algorithm description
The cloud screening and cloud masking is performed using the NWC SAF MSG v2010 algorithm, which is described in more detail in [RD 1]. See http://NWC SAF.org for details on the NWC-SAF project. The algorithm is based on a multi-spectral thresholding technique applied to every pixel of the satellite scene (Derrien and LeGleau, 2005 and 2010). Several threshold tests may be applied and must be passed before a pixel is assigned to be cloudy or cloud-free.

Thresholds are determined from present viewing and illumination conditions and from the current atmospheric state (prescribed by data assimilation products from numerical weather prediction models – here, the ERA-Interim dataset, see Dee et al, 2011 and http://www.ecmwf.int/research/era/do/get/era-interim).

Highlights

- Cloud screening is based on information from SEVIRI channels R0.6µm, R0.8µm, R1.6µm, T3.9µm, T8.7µm, T10.8µm, T12.0µm, T13.4µm
- The cloud masking algorithm delineates all cloud-free pixels in a satellite scene with a high confidence, see [RD 2].
- Different tests are applied, where it is distinguished between land or sea pixels, in the following the solar illumination (daytime, night-time, twilight, sunglint) and the viewing angles are criteria for the application of a certain test.
- Daytime conditions with good illumination (i.e, conditions enabling access to information in all spectral channels) provide best cloud screening results
- Transition between day- and night-time is smoothed with the temporal dependence twilight test (Derrien and LeGleau, 2010)

Limitations

- Not all clouds will be detected due to inherent limitations of the SEVIRI imager as being a passive radiometer with a rather coarse field of view (here 3 x 3 km² at sub-satellite point). This can be compared to actively probing instruments (like cloud lidars and radars) with a much higher cloud detection sensitivity. Better agreement between Calipso and SEVIRI was found when clouds with an optical depth smaller 0.3 were removed from the Calipso dataset.
- Some thin clouds (particularly, ice clouds) over cold ground surfaces may remain undetected even if having cloud optical thicknesses higher than the above mentioned detection limit
- The cloud detection algorithm changes from VIS/IR to an infrared only version at the transition from day to night. Even though we applied the SAF NWC msgv2010 package with a special twilight transition procedure, the switch from day- to night-time algorithm remains present. Irregularities can occur as spikes in the diurnal cycle.
- Since SEVIRI is mounted on geostationary satellites, a distinct dependency on viewing zenith angle occurs that leads to an overestimating of cloudiness at high VZA
- Furthermore no attempt is made to take into account that pixels labeled as being only cloud-contaminated are not totally covered by clouds. This means that the SEVIRI CFC values will generally slightly overestimate cloud amounts. The overestimation is largest over ocean surfaces and may be as high as 10 % in absolute CFC units.
- An underestimation for small VZA is found by comparing with SYNOP and MODIS

Validation

CLAAS CFC was validated in detail with independent data sets very different in nature and in different stages of processing, see RD 1 for a complete analysis. The results can be summed up as follows. Coverage of the complete SEVIRI disk with ground based observations was realized by using SYNOP as database, on average SEVIRI monthly mean is 2.7 % (absolute value) higher than the SYNOP monthly mean. CFC was also validated against the comparable instrument MODIS which is considered to be the most advanced and best explored passive sensor in space, also in this case an overestimating of monthly mean cloud cover by SEVIRI

was found, though very small (1.7 %). Finally, the cloud mask was compared with A-train measurements acquired with active sensors, the cloud profiling radar CPR and the lidar CALIOP. The probability of detecting a cloud was found to be 0.9012 for CPR and 0.9271 in case of CALIOP, where clouds with an optical depth smaller than 0.3 were removed from the CALIOP data.
As a last step, also the previous operationally produced SEVIRI CFC was considered concerning the transition from day- to night-time. The transition zone is generally smoother in the CLAAS dataset than in the operational version.
CLAAS CFC fulfils threshold and target requirements (10% bias and 20% absolute precision for monthly means or 15% and 20% for daily means respectivley, see RD 1) in all cases. Also the optimal accuracy, which is 10% bias and 15% absolute precision for both, daily and monthly means, is achieved for comparison with both, ground-based as well as space-borne derived data sets.
From the SYNOP data, that we consider to be stable over time, it was demonstrated that no artificial trends occur when changing from MSG 1 to MSG 2.
Since SEVIRI is mounted on geostationary satellites, a distinct dependency on viewing zenith angle (VZA) occurs that leads to an overestimating of cloudiness at high VZA. However also a distinct underestimation for small VZA is found by comparing with SYNOP . Accurate evaluation is difficult in this case since the number of observations is low in the regions in question and single stations might not be trustworthy. Nevertheless MODIS comparisons confirm the SYNOP results to some extent, but the underestimation amounts to only half of the SYNOP deviation.

Recommended applications

The product can be used everywhere except at the rims of the disk, CFC values at viewing zenith angles larger than 75° are too high and become unreliable. Of course the users can decide by themselves with the help of the validation report [RD 1].

Possible applications of cloud fractional cover are all those which require multi annual, stable and spatiotemporally highly resolved CFc values. Tracking of convective cloud systems like thunderstorm fields (Goyens *et al*., 2011) or monitoring convective initiation in middle Europe (Siewert *et al*., 2010) shall serve as an example here.

Further reading

More details on the product retrieval are given in [RD 1] and [RD 3]. Information on the achieved accuracy and precision of the product is found in the CM SAF SEVIRI validation report [RD 1].

4.1.2 Cloud Top level – CTO

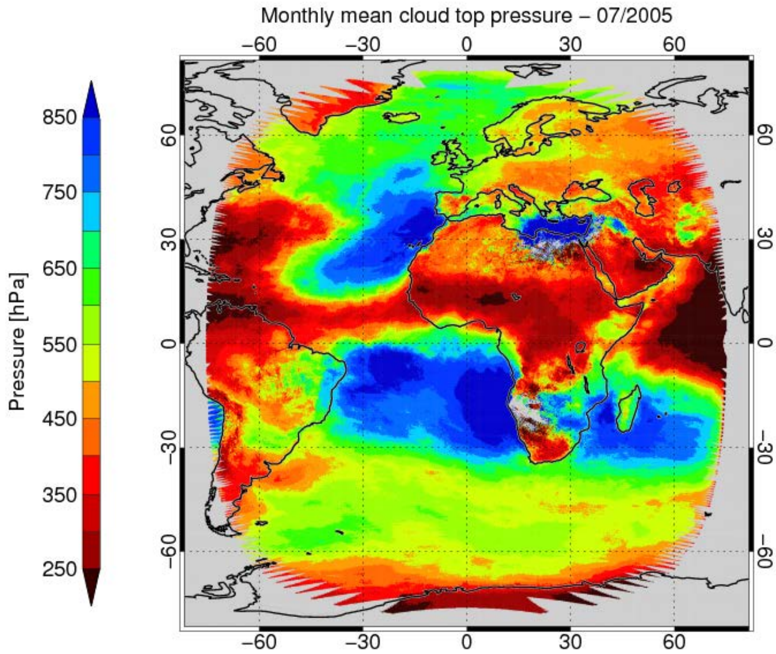

Figure 4-2: *SEVIRI monthly mean cloud top pressure for July 2005.*

Three versions of the CLAAS Cloud Top product exist:

1. The Cloud Top Temperature (CTT), expressed in Kelvin
2. The Cloud Top Height (CTH), expressed as altitude (m) relative to topography.
3. The Cloud Top Pressure (CTP), expressed in pressure co-ordinates (hPa).

Notice that the cloud altitude given by CTH is defined as the mean cloud altitude relative to the mean sea level.

Daily and monthly average products are calculated by averaging the original algorithm output in SEVIRI pixel resolution for all available scenes. All products are averaged arithmetically (linearly) but for the Cloud Top Pressure product also a geometric mean (i.e., average of the logarithm of cloud top pressure) is available. An example of the Cloud Top Pressure product can be found in Figure 4-2.

Short Algorithm description
For the determination of cloud top information, the NWC SAF algorithms are used, details can be found in [RD 1]. The algorithm is applied to all cloudy pixels as identified by the SAF NWC msgv2010 cloud mask product.
In a first step, cloudy pixels are separated into three classes depending on cloud type or its opacity respectively: 1) very low, low or medium thick as well as middle level clouds, 2) high opaque clouds and 3) high semi-transparent clouds.
Using RTTOV (http://research.metoffice.gov.uk/research/interproj/nwpsaf/rtm/) the corresponding radiances and brightness temperatures for overcast and clear sky are simulated

for each pixel, with vertical profiles of temperature and humidity analysis from ERA-Interim (Dee et al., 2012) as ancillary input. The SEVIRI channels used are: 6.2, 7.3, 13.4 10.8, 12.0 µm.
For very low, low or medium thick clouds as well as opaque clouds the cloud top pressure is retrieved as the best fit between the simulated and the measured 10.8µm brightness temperatures. Also the possibility of a low level thermal inversion is taken into account with the help of the ERA-Interim temperature profile at the respective pixel . In that case the very low, low or medium clouds are assumed to form at the inversion level, while they can also rise above that level if their brightness temperatures are colder than the air temperature below the thermal inversion. The type of the inversion (dry air above the inversion level or not) is included by subtracting a variable offset.
In case of semitransparent clouds the radiance rationing method is used, in which the ratio of radiances from 2 channels is compared to simulated radiances at clear sky conditions for a fixed temperature profile or H2O/IRW intercept method. For the latter a linear relationship of radiance between 2 spectral bands is assumed, but a curve for a window and a sounding channel. For opaque clouds this technique is always applied as preceding test, in order to remove any pixels that are semitransparent but where in fact falsely labeled as opaque by the cloud type test.

Highlights

- Cloud top heights are determined using the reference profiles available from the ERA-Interim dataset. The ERA-interim fields have been spatially remapped to a pre-defined grid covering the SEVIRI disc. During run time, the vertical profiles used are temporally interpolated to the exact slot time using the two nearest in time spatially remapped ERA-Interim fields.
- The applied techniques used to derive CTO are chosen depending on the cloudy pixel's type. The cloud type was assigned in a preparation step prior to the actual CTO-algorithm.
- In case of a thermal inversion in the ancillary NWP fields, the clouds are usually positioned at this inversion. However, very low, low or medium clouds can also rise above the inversion level if their brightness temperatures are colder than the air temperature below the thermal inversion. The method accounts also for the atmospheric state above the inversion level (dry air above the inversion level or not)

Limitations

- The quality of the CTO product depends to some extent on the quality of the reference vertical profiles of temperature and moisture taken from NWP model analyses. Especially troublesome is the treatment of situations with temperature inversions since this implies that there are several solutions to the problem of matching measured cloud top temperatures to vertical reference profiles. Details of the impact of varying NWP information on CTO products are included in the visiting scientist study from Trolez et al. (2008). Also a direct comparison of the influence of ERA Interim input compared to GME input for the SEVIRI cloud top retrieval was undertaken in Fuchs (2012).
- Cloud top pressure is erroneous if clouds were assigned a wrong type, this results for example in an underestimation of cloud top height/pressure for semi-transparent clouds classified as low/medium or an over estimation of cloud top height/pressure for low/medium clouds classified as semi-transparent

- CTO is not retrieved for pixel that are not fully cloudy but were classified as cloud contaminated
- As mentioned for the CFC product, optically very thin clouds may not be detected at all.
- Clouds interpreted as being opaque are in reality often diffuse or multi-layered in their upper portions – this often leads to an underestimation of the true cloud top of up to 2000 m

Validation

CLAAS CTO was validated with both, the ground-based radar MIRA at Lindenberg as well as the space-born cloud profiling radar CPR on CloudSat, with MODIS and also CALIOP. Comparisons were made at Level 2 and Level 3 stage of data processing.

CTH meets threshold as well as target accuracy in all cases, where the target accuracy is 800 m (bias) or 1500 m precision, respectivley. The optimal requirement of 500 m concerning accuracy is also achieved for Cloudnet and CALPSO/CPR comparisons.

CTP was compared with MODIS CTP, revealing that SEVIRI CTP was often lower, mainly in the tropical region. Since the MODIS monthly mean product has a poor smapling of maxmila 4 measurements per day, the diurnal cycle of CTP is not very well represented. Nevertheless, a further analysis concerning this issue in the specific regions did not deliver an explanation. The comparisons for the cloud top (see below) did not confirm these large differences. But when comparing the joint histograms, a portion of high clouds appears that is not as much pronounced in the reference datasets, especially in case of ice clouds. This might indicate an uncertainty in cloud phase detection

CTH: Validation with CPR and CALIOP led to best agreement with CPR, which shows, that both sensors are equally insensitive to high thin cirrus. Those are detected by CALIOP and so the comparison with CALIOP was carried out in two modes: with and without filtering of thin cloud layers, the latter to mimic the sensitivity of a passive sensor. This led to an improvement in agreement.

The Cloudnet time-series of CTH possesses a clear positive trend that is not observed for SEVIRI data. This trend is considered to be artificial due to an upgrade of the radar system in 2010.

Recommended applications

For CTO, similar recommendations as for the CFC products (see above) are given, concerning the applicability at high viewing zenith angles.

Possible applications of CTO are all those which require multi annual, stable and spatiotemporally highly resolved CTO values. It is possible for example to study the travelling of the inner tropical convergence zone throughout the years (Kniffka *et al.*, 2010) or facilitate research on transition from one cloud development stage to another, such as the transition from stratocumulus to cumulus.

Further reading

More details on the product retrieval are given in [RD 1] and [RD 3]. Information on the achieved accuracy of the product is found in the CM SAF SEVIRI validation report [RD 1.] and the CM SAF service specification [AD 2].

4.1.3 Cloud Optical Thickness – COT

Short Algorithm description

The central principle of the method to retrieve cloud physical properties is that the reflectance of clouds at a non-absorbing wavelength in the visible region (0.6 or 0.8 μm) is strongly related to the optical thickness and has little dependence on particle effective radius (r_e), whereas the reflectance of clouds at an absorbing wavelength in the near-infrared region (1.6 or 3.7 μm) is strongly dependent on effective radius (Nakajima and King, 1992).

In the CPP v3.9 algorithm (Roebeling et al. 2006), the Doubling-Adding KNMI (DAK) radiative transfer model (De Haan et al. 1987 and Stammes 2001) is used to simulate 0.6- and 1.6-/3.7-μm top-of-atmosphere reflectances as a function of viewing geometry, cloud optical thickness, effective radius, and cloud phase. These simulated reflectances are stored in a look-up table (LUT).

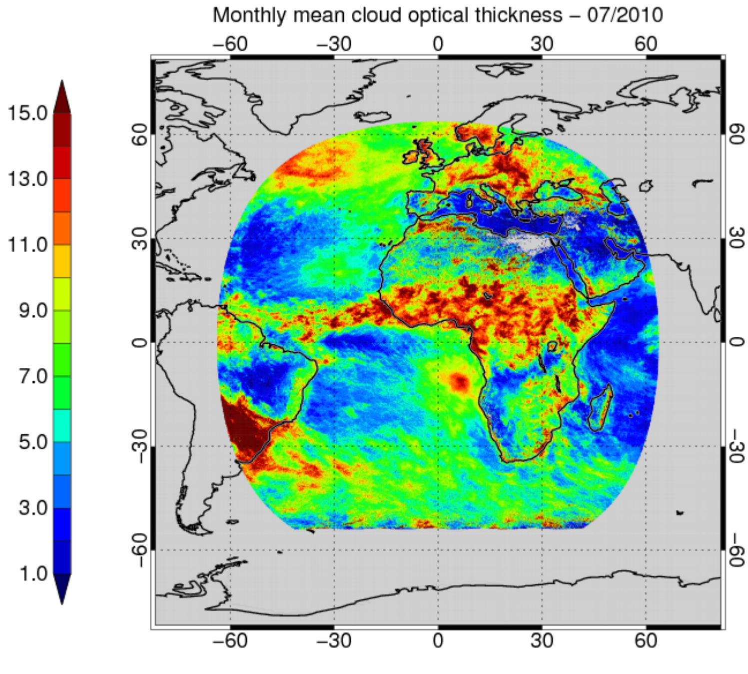

Figure 4-3: *Monthly mean cloud optical thickness from SEVIRI on MSG 2, July 2010.*

COT and r_e are retrieved for cloudy pixels in an iterative manner by simultaneously comparing satellite-observed reflectances to the LUT of RTM-simulated reflectances. The iteration process continues until the retrieved cloud optical thickness converges to a stable value. See Figure 4-6 for an example of a monthly mean COT field.

Highlights

- An estimate of the COT retrieval error is reported.
- The careful calibration of SEVIRI's VIS channels takes effect particularly in the retrieval of microphysical properties
- The effect of absorption by trace gases in the atmosphere on narrowband reflectances is taken into account using MODTRAN (Berk et al. 2000) simulations (Meirink et al. 2009).

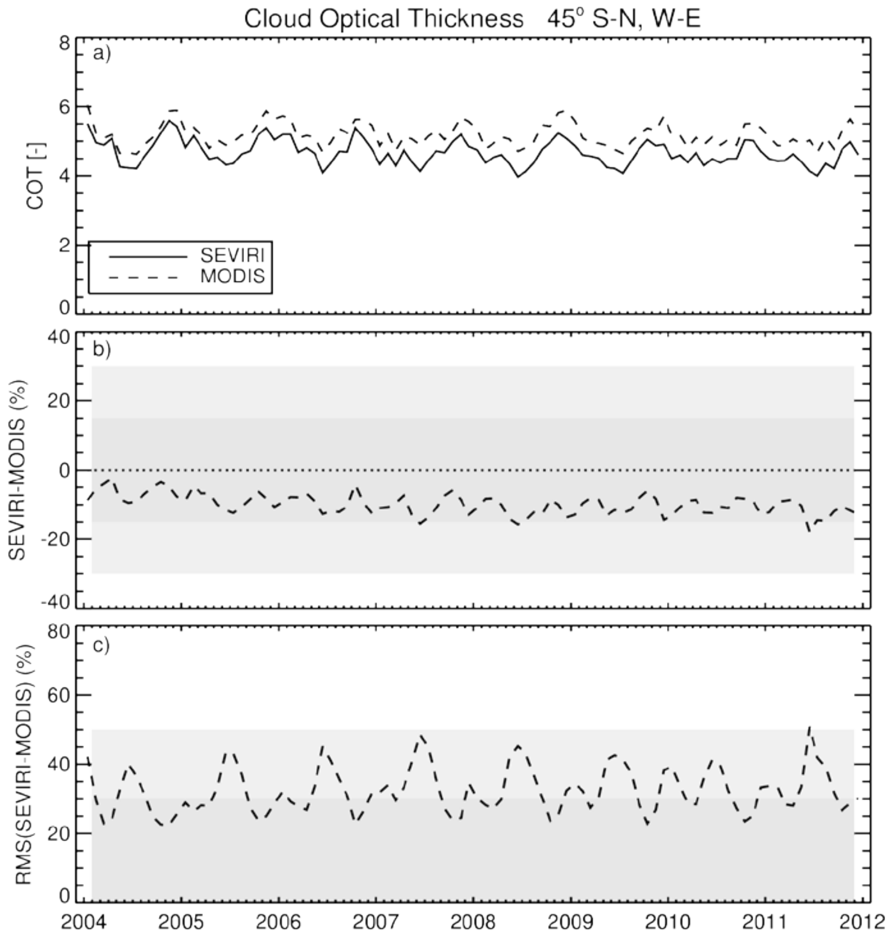

Figure 4-4: *Time series of COT, including bias and rms compared to MODIS.*

Limitations

The main limitations of the COT retrieval are:

- The derivation of cloud physical properties from reflected solar radiation is dependent on the availability of daylight. This means that no retrievals can be done during night time. In practice a maximum solar zenith angle of 72 degrees is allowed.
- Due to the viewing geometry of geostationary satellites the derivation of microphysical properties was restricted to VZA < 72°
- The retrieval is highly problematic over very bright surfaces, particularly ice and snow, as the visible reflectance from clouds is similar to that from the surface.

- Cloud property retrievals are performed assuming that clouds are plane parallel. Two prominent examples of cases for which this assumption is violated are: (1) three-dimensional radiative effects become important if large sub-pixel variations in cloud-top height occur, and particularly if the solar zenith angle is large; (2) retrievals for broken clouds are affected by a reflectance contribution from the surface, usually leading to an underestimation in COT compared to the cloudy portion of the pixel.
- Aerosols are not considered in the CPP retrieval. This assumption is usually justified because aerosols reside below or within the cloud and their optical thickness is small compared to that of the cloud. However, if the aerosols reside above the cloud and if they are sufficiently absorbing, they can significantly lower the visible reflectance. This leads to an underestimation of COT.

Validation results

All microphysical properties of clouds detected by SEVIRI were compared to MODIS where we generated Level 3 products from Level 2 data to ensure comparability of the datasets. The analysis was restricted to -45° < latitude < 45° since microphysical products are only derived at daylight conditions and so the database is maximised.
Threshold requirements are met for COT for bias and precision (25% and 50%). Target requirement of 10% is equally met for the bias.
In Figure 4-4 the time-series of COT for the complete SEVIRI dataset as well as a the bias and rms compared to MODIS can be found. SEVIRI detects in general thinner clouds than MODIS for all month, the bias shows no seasonal cycle while the rms exhibits an observable dependency on the season.
The complete validation of all microphysical parameters can be found in RD 1.

Recommended applications

The COT dataset is most reliable at lower latitudes, or (better said) lower solar zenith angles (below about 65 degrees). In addition, high latitudes are frequently affected by snow and ice cover. In these cases retrievals are problematic, even more because our ancillary database currently does not represent snow and ice cover well. Also, the viewing angle of SEVIRI should be small enough, to inhibit cloud geometry errors. Therefore we restricted the derivation of microphysical properties to VZA < 72° like the maximum SZA! In the data fields these regions will appear as no data pixel, see e.g. the regions shaded in grey in Figure 4-3.
In general, COT can be applied where multi annual, stable and spatiotemporally highly resolved information is needed. Analysis of the detection of Cd/Tcu clouds is mentioned here as an example (Carbajal Henken *et al*., 2011).

Further reading

More details on the product retrieval are given in [RD 1] and [RD 4]. Information on the achieved accuracy of the product is found in the CM SAF SEVIRI validation report [RD 1] and the CM SAF service specification [AD 2].

4.1.4 Cloud Phase – CPH

Short Algorithm description

Cloud phase is interpreted primarily using reflected solar radiation in the 0.6 and 1.6/3.7 µm channels. At 0.6 µm, both liquid water and ice have very small values of the imaginary index of refraction, which determines the amount of absorbed solar radiation. At 1.6 and 3.7 µm, the imaginary index of refraction is higher for ice particles than for liquid particles, thus a smaller reflectance will be measured from ice clouds. As a result, these channels are useful to distinguish water from ice clouds (see e.g. Baum et al., 2000).

Water and *ice* are assigned to those cloud-flagged pixels for which the measured 0.6-µm and 1.6/3.7-µm reflectances correspond to the respective simulated LUT reflectance. Since visual image inspection revealed that ice is erroneously assigned to optically thin water clouds (e.g.

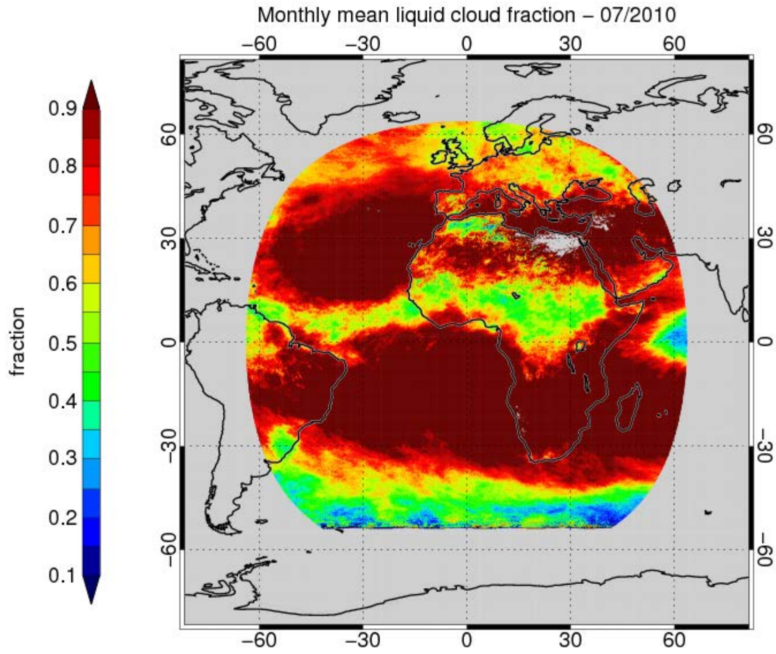

Figure 4-5: *Fraction of liquid clouds detected by CPP, monthly average for July 2010.*

at the edges of cloud fields), an empirical cloud-top temperature (CTT) check, based on measured 10.8-µm brightness temperature, was included. The CTT is not taken from the official CM SAF product because this contains no-data values for some cloudy pixels. Instead, the cloud-top temperature is obtained by correcting for cloud emissivity less than unity, using the ratio of visible to infrared cloud optical thickness and neglecting thermal infrared scattering (Minnis et al., 1993). If the *ice* phase has been retrieved initially, but the cloud top temperature is higher than 265 K, the phase is set to *water*.

Currently, the output values of the CPH product are *ice* and *water*, i.e.: *mixed* phase is not retrieved by this method. For an example of the cloud phase see Figure 4-5, here the monthly mean of the liquid cloud fraction from July 2010 is displayed.

Highlights

- The algorithm uses near-infrared reflectances and an additional cloud-top temperature check to detect cloud phase.
- The algorithm performs well in comparison with ground-based observed cloud phase over Cabauw, The Netherlands (Wolters et al. 2008).

Limitations

The main limitations of the CPH retrieval are:

- The derivation of cloud physical properties from reflected solar radiation is dependent on the availability of daylight. This means that no retrievals can be done during night time. In practice a maximum solar zenith angle of 72 degrees is allowed.
- The retrieval is highly problematic over very bright surfaces, particularly ice and snow, as the visible reflectance from clouds is similar to that from the surface.
- In case of thin ice clouds over water clouds, the visible and near-infrared reflectances are dominated by the water cloud layer, which results in an erroneous *water* labeling. Validation results indicate that the water cloud occurrence might be overestimated by almost 100% at the expense of the corresponding ice cloud occurrence. The largest overestimations occur in case of very thin ice clouds over thick water clouds. Wolters et al. (2008) have shown that these overestimations rapidly decrease with increasing ice cloud optical thickness, and are less than 10% in case of ice clouds with COT > ~1.
- Erroneous ice phase retrievals might occur in case of broken or inhomogeneous overcast clouds, in particular over ocean surfaces. However, this concerns only about 3% of the cloud-phase retrievals (Wolters et al., 2010).

Validation

Thermodynamic phase is analysed in RD 1 in terms of the fraction of liquid clouds relative to the total cloud fraction. The multi-year mean liquid cloud fraction is compared with MODIS in Figure 4-6. There are two MODIS phase products: the Infrared (IR) and the Optical Properties (OPT). The CLAAS phase agrees best with the MODIS-IR product. On average, the bias of CLAAS phase against MODIS-IR is small and easily within the target requirement of 0.05. The same holds for the RMS, where the target requirement is 0.1. The deviations with respect to MODIS-OPT are larger but still within the threshold requirements. There are hints for a small negative trend in MODIS-IR phase.

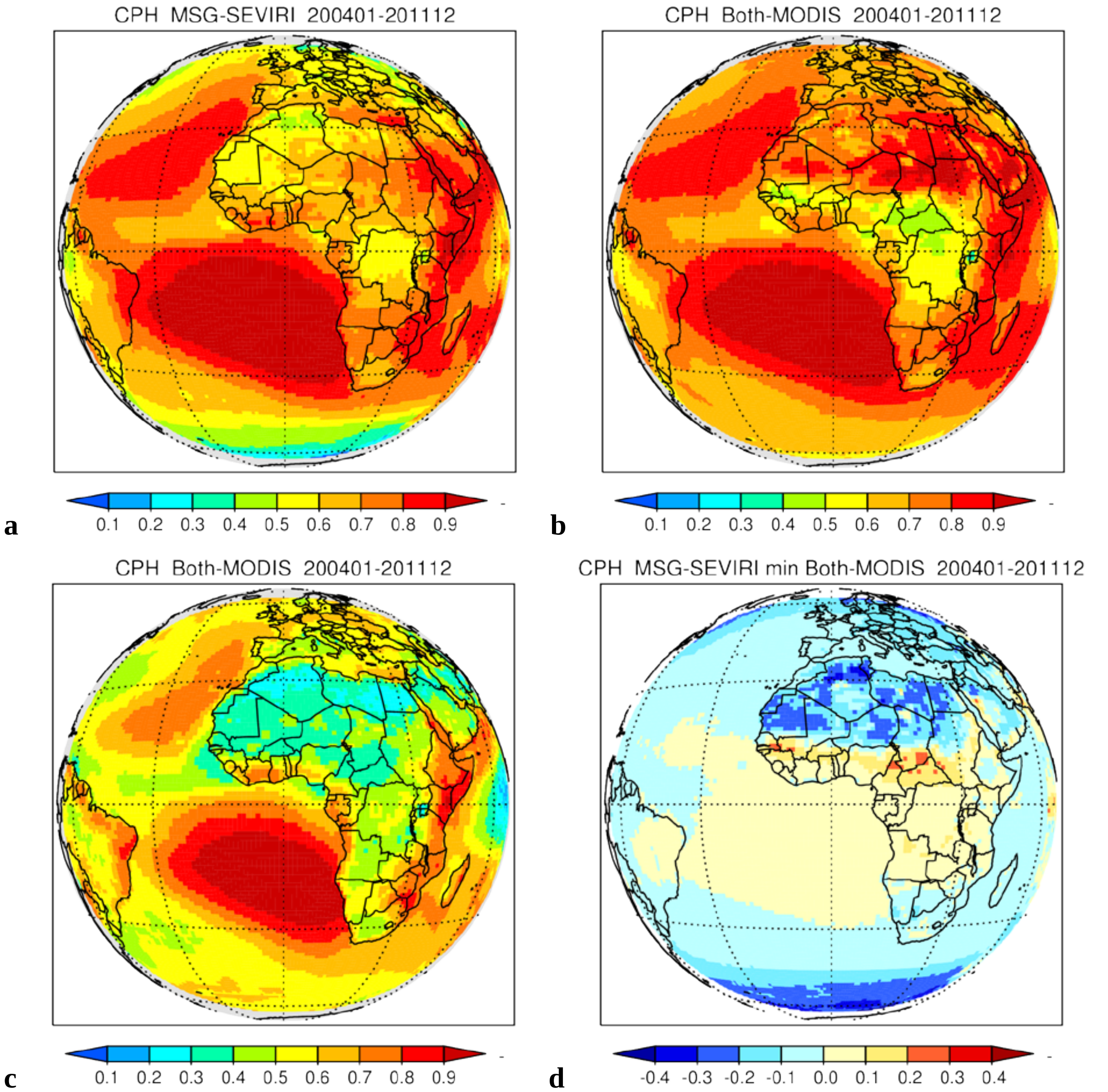

Figure 4-6: Fraction of liquid clouds (relative to total cloud fraction) averaged from January 2004 until December 2011: (a) CLAAS, (b) MODIS Infrared product, (c) MODIS optical properties product, and (d) difference between CLAAS and MODIS Infrared product.

Recommended applications

The CPH dataset is most reliable at lower latitudes, or (better said) lower solar zenith angles (below about 65 degrees). In addition, high latitudes are frequently affected by snow and ice cover. In these cases retrievals are problematic, even more because our ancillary database currently does not represent snow and ice cover well. Also, the viewing angle of SEVIRI should be small enough, to inhibit cloud geometry errors. Therefore we restricted the derivation of microphysical properties to VZA < 72° like the maximum SZA! In the data fields these regions will appear as no data pixel, see e.g. the regions shaded in grey in Figure 4-7.

Wherever multi annual, stable and spatiotemporally highly resolved information is needed, CPH data from SEVIRI can be applied. Analysis of the detection of Cd/Tcu clouds is mentioned here as an example (Carbajal Henken et al., 2011).

Further reading

More details on the product retrieval are given in [RD 1] and [RD 4]. Information on the achieved accuracy of the product is found in the CM SAF SEVIRI validation report [RD 1] and the CM SAF service specification [AD 2].

4.1.5 Liquid Water Path – LWP

Short Algorithm description

Cloud optical thickness (τ) and droplet effective radius (r_e) are retrieved simultaneously using CPP. From these two properties, the cloud water path (CWP) of water clouds (or liquid water path, LWP) can be computed using the following relation (Stephens, 1978):

$$CWP = 2/3\ \rho_l\ \tau\ r_{e},$$

where ρ_l is the density of liquid water. For water clouds effective radii between 1 and 24 µm are retrieved.

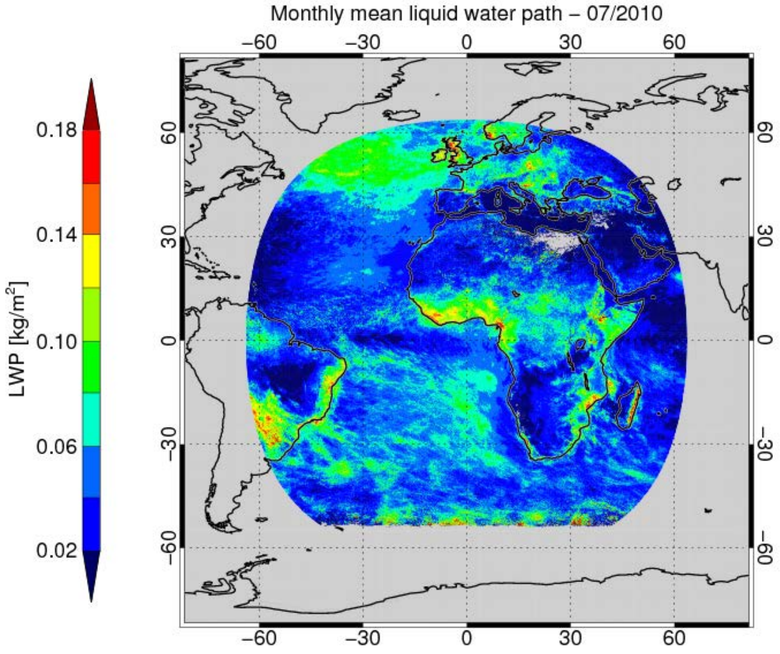

Figure 4-7: Liquid water path as seen by SEVIRI, monthly average for July 2010.

Highlights

- LWP is calculated from the product of the COT and cloud particle effective radius retrieval.
- An estimate of the LWP retrieval error is reported.
- Evaluation with ground-based microwave radiometer-derived LWP at Cloudnet sites showed good agreement (Roebeling et al. 2008).

Limitations

The main limitations of the LWP retrieval are:

- The derivation of cloud physical properties from reflected solar radiation is dependent on the availability of daylight. This means that no retrievals can be done during night time. In practice a maximum solar zenith angle of 72 degrees is allowed.
- LWP is calculated from COT and r_e. This implies that all limitations for COT mentioned in Section 4.1.3 are also limitations for LWP.
- Unlike active satellite instruments, which can derive cloud profile information, retrievals from passive satellite instruments are limited by the fact that the obtained signal emanates from the integrated profile. Since near-infrared radiation is only penetrating into the cloud to a certain depth (due to absorption by cloud particles), the retrieved cloud phase and effective radius are representative for the upper part of the cloud (Platnick 2001). The penetration depth depends on the amount of absorption by cloud particles, which is increasing with wavelength. This means that the retrieved CPH and r_e depend on which NIR spectral channel is used (in our case 1.6 or 3.7 μm).
- In the derivation of Equation (2) for LWP it is assumed that the cloud particle effective radius does not vary with height. In reality this assumption is not satisfied. For example, liquid water clouds often obey adiabatic theory leading to a slightly different relation for LWP, in which the factor 2/3 is replaced by 5/9.
- Regarding the case of aerosol layers above clouds, the effect of these aerosols on the retrievals depends on the channel combination used and on the aerosol properties (Haywood et al. 2004). The impact is strongest for the 1.6-μm channel, with a possible underestimation of r_e by several microns. For the 3.7-μm channel, the impact is smaller and can be an overestimation of r_e.
- Because the retrieval of effective radius becomes unreliable for thin clouds, weighting with a climatological average r_e is performed for clouds with COT < 8 (COT < 5) in case the 1.6-μm (3.7-μm) channel is used. Although this stabilizes the retrieval results, it does not take away the inherent uncertainty in r_e retrievals for thin clouds.

Validation

Multi-year mean spatial distributions and area-averaged time series of CLAAS all-sky liquid water path are compared with MODIS, see Figure 4-8 The CLAAS and MODIS LWP spatial distributions agree very well at latitudes below about 40 to 50 degrees. Specific regions with high LWP along parts of the west coast of Africa and east coast of South-America can be consistently observed in both datasets. At high latitudes MODIS LWP increases considerably, similar to what was observed for COT. CLAAS all-sky LWP is up to 50% smaller than MODIS at high latitudes, which is roughly consistent with its 50% smaller liquid cloud fraction. This implies that in-cloud LWPs are in much closer agreement. In the relative difference plot, the South-Atlantic trade cumulus region stands out (apart from the nearly cloud-free deserts). This region is characterized by a large fraction of broken clouds, leading to many MODIS pixels being restored to clear-sky and consequently a lower all-sky LWP.

The CLAAS and MODIS time series are in very good agreement, with a nearly identical seasonal cycle. The bias is within the target requirement of 10%, while the RMS does not reach the 25% target but is within the threshold requirement of 50%.

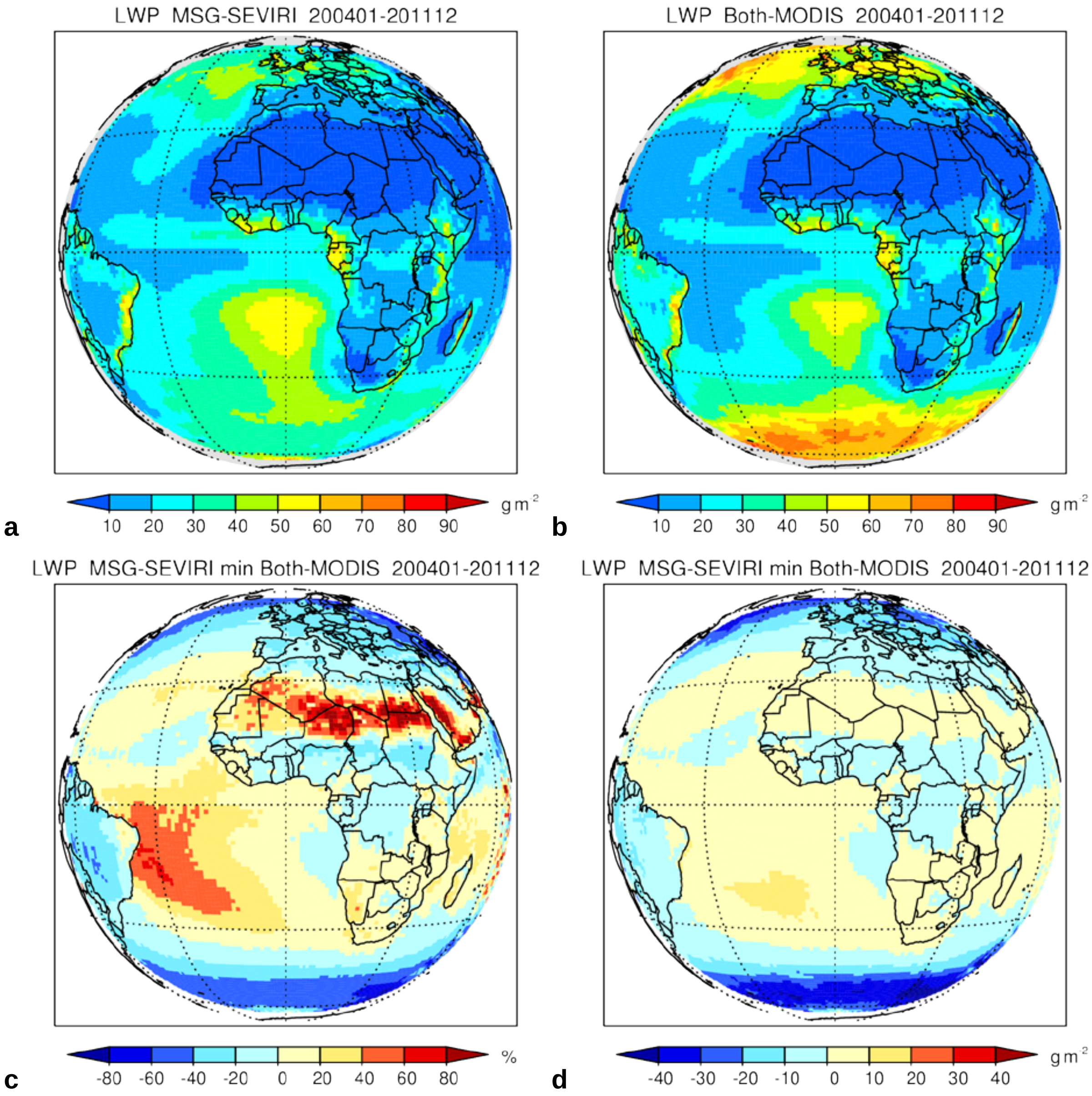

Figure 4-8: All-sky liquid water path averaged from January 2004 until December 2011: (a) CLAAS, (b) MODIS, (c) relative difference between CLAAS and MODIS, and (d) absolute difference between CLAAS and MODIS.

Recommended applications

The LWP dataset is most reliable at lower latitudes, or (better said) lower solar zenith angles (below about 65 degrees). In addition, high latitudes are frequently affected by snow and ice cover. In these cases retrievals are problematic, even more because our ancillary database currently does not represent snow and ice cover well. . Also, the viewing angle of SEVIRI should be small enough, to inhibit cloud geometry errors. Therefore we restricted the derivation of microphysical properties to VZA < 72° like the maximum SZA! ! In the data fields these regions will appear as no data pixel, see e.g. the regions shaded in grey in Figure 4-7.

In general, use of LWP is feasible where multi annual, stable and spatiotemporally highly resolved information is needed. Model evaluation of the diurnal cycle of cloud water path is one of the possible applications, see Roebeling and van Meijgaard (2009).

Further reading

More details on the product retrieval are given in [RD 1] and [RD 4]. Information on the achieved accuracy of the product is found in the CM SAF SEVIRI validation report [RD 1] and the CM SAF service specification [AD 2].

4.1.6 Ice Water Path – IWP

Short Algorithm description

The CWP for ice clouds (or Ice Water Path, IWP) is approximated using the same relation as for LWP but with COT and r_e retrievals based on RTM simulations for imperfect hexagonal ice crystals. Homogeneous distributions of C0, C1, C2, and C3 type ice crystals from the COP library (Hess et al., 1998) are assumed, with effective radii of 6, 12, 26, and 51 µm, respectively. The average IWP for July 2010 is shown as an example in Figure 4-9.

Highlights

- The use of imperfect hexagonal ice crystals gives reasonably adequate simulations of total and polarized reflectance of ice clouds, outperforming more complex ice crystal habits in many cases (Knap et al. 2005).
- An estimate of the IWP retrieval error is reported.

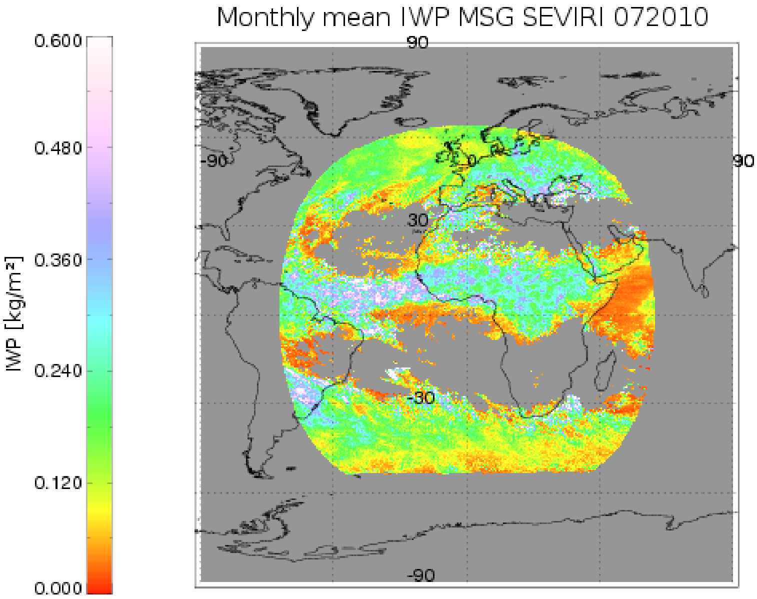

Figure 4-9: *Monthly average of ice water path as seen by SEVIRI, July 2010.*

Limitations

The same limitations as for LWP hold also for IWP. In addition, the r_e retrieval for ice clouds is considerably more uncertain than for water clouds, because particle shapes and roughness vary widely and are not well known. The assumptions on ice crystal habits used to generate the LUTs (in our case imperfect hexagons are assumed) have a profound impact on the retrieved r_e and IWP.

Validation

Multi-year mean spatial distributions and area-averaged time series of CLAAS all-sky ice water path were compared with MODIS. As for LWP there is a remarkable agreement in the spatial patterns, especially along the ITCZ, see Figure 4-10. Also, IWP gets much higher for MODIS than for CLAAS at high latitudes. This contrasts with a lower MODIS ice cloud fraction in that area, implying that the in-cloud IWP difference is even larger. At lower latitudes and far to the west, where solar zenith angles are low but SEVIRI viewing angles are high, there are also signs of CLAAS IWP being lower than MODIS.

The seasonal cycles of CLAAS and MODIS IWP agree very well, and the bias is within the optimal requirement of 10%, while the rms reaches the target requirement of 40% (see [RD 1]).

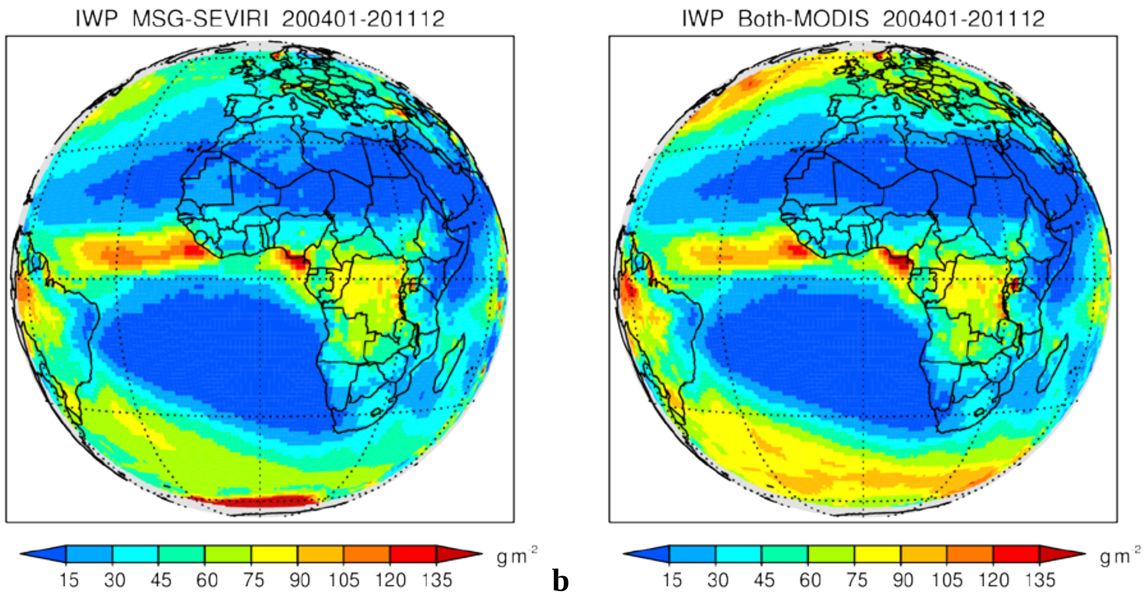

a **b**

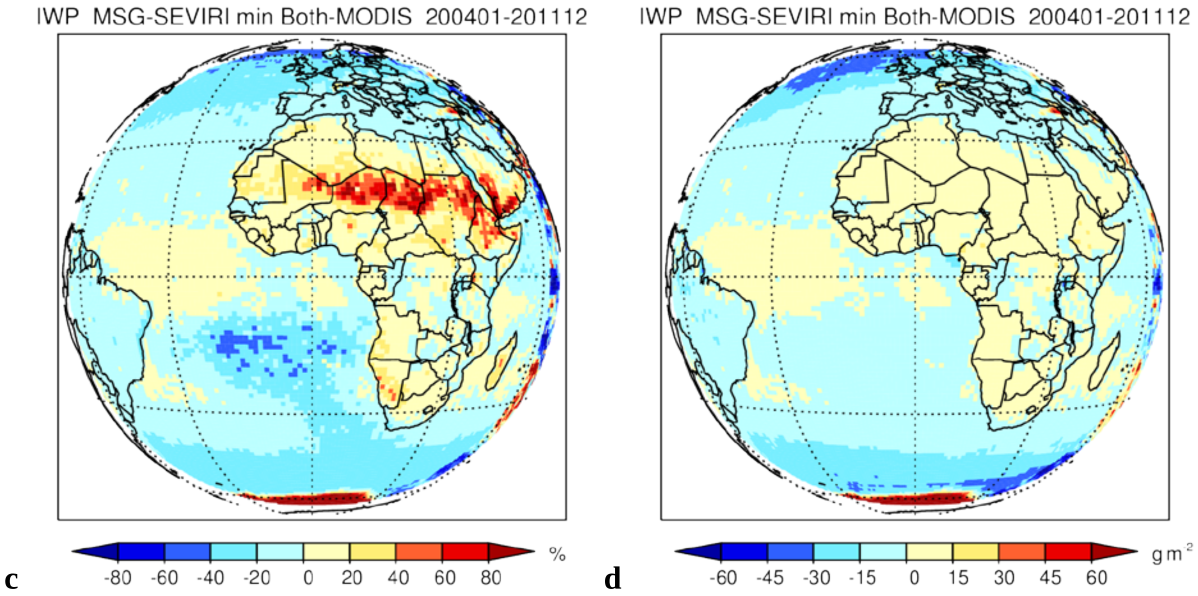

Figure 4-10: All-sky ice water path averaged from January 2004 until December 2011: (a) CLAAS, (b) MODIS, (c) relative difference between CLAAS and MODIS, and (d) absolute difference between CLAAS and MODIS.

Recommended applications

The IWP dataset is just like LWP most reliable at lower latitudes, or lower solar zenith angles below about 65 degrees. In addition, high latitudes are frequently affected by snow and ice cover. In these cases retrievals are problematic, even more because our ancillary database currently does not represent snow and ice cover well. . Also, the viewing angle of SEVIRI should be small enough, to inhibit cloud geometry errors. Therefore we restricted the derivation of microphysical properties to VZA < 72° like the maximum SZA! ! In the data fields these regions will appear as no data pixel, see e.g. the regions shaded in grey in Figure 4-9.

IWP can like LWP be applied where multi annual, stable and spatiotemporally highly resolved information is needed. Model evaluation of the diurnal cycle of cloud water path is one of the possible applications, see Roebeling and van Meijgaard (2009).

Further reading

More details on the product retrieval are given in [RD 1 and [RD 4]. Information on the achieved accuracy of the product is found in the CM SAF SEVIRI validation report [RD 1] and the CM SAF service specification [AD 2].

4.1.7 Joint Cloud property Histograms – JCH

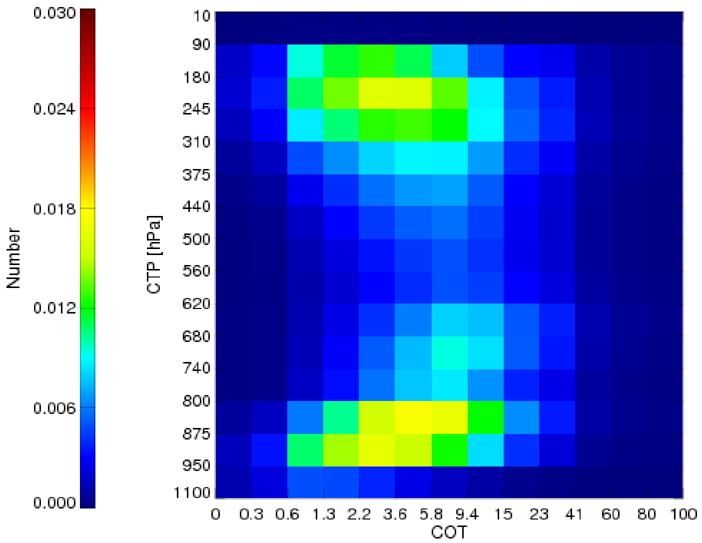

Figure 4-11: *JCH, a 2D histogram of cloud top pressure and cloud optical thickness, here aggregated over the complete SEVIRI disk for 03/2004.*

Short Algorithm description

The JCH product is a combined histogram of CTP and COT covering the solution space of both parameters. This two-dimensional histogram gives the absolute numbers of occurrences for specific COT and CTP combinations defined by specific bins. More details on this product can be found in [RD 5], an example of JCH for March 2004 is shown in Figure 4-11.

Highlights

- The product adds value to the single standard Level 3 products of CTP and COT by showing how the two parameters vary together
- The histograms are given for each grid point which means that a user can aggregate results over any local or regional domain in order to analyse typical cloud regimes (or types)
- The use of joint histograms is common in applications for evaluating climate models (see http://cfmip.metoffice.com/COSP.html)

Limitations

- The product is only available during daytime since the COT parameter is not retrieved at night

More details on the product retrieval are given in [RD 1.] and [RD 5]. Information on the achieved accuracy of the product is found in the CM SAF SEVIRI validation report [RD 1] and the CM SAF service specification [AD 2].

Recommended applications

With the JCH diagrams the discrimination between different cloud regimes is supported. COT and CTP information can readily be considered in a more statistical way.

Since the CM SAF JCH product is compiled as distributions for each grid point, it is possible to compose cloud distribution statistics for any region size on the globe by simple aggregation of grid point values.

5 Outlook

The present CLAAS dataset is the first complete processing of the SEVIRI time-series from 2004 – 2011 by CM SAF. In CDOP 2 (the next phase of the CM SAF project) a new version of the SEVIRI data set will be processed. The experience that we gained while creating and evaluating this first edition will be incorporated into the next dataset version.

Some new features will be:

- The applied algorithms will be updated after a careful testing of performance and quality
- The possibility of including error characteristics of the processed variables will be explored
- The temporal resolution of the next dataset will be increased to 15 minutes, so the full dataset of SEVIRI will be utilized. This will further improve the accuracy of the diurnal cycle of the processed variables. Especially in case of CFC, fast moving clouds will be visible which also enables to use the NWC SAF cloudmasking algorithm to its full capacity
- The length of the dataset will be increased
- A new temporally variable version of the VIS/NIR calibration will be applied, also an infrared calibration will be explored and eventually integrated

While processing CLAAS some specific shortcomings were encountered. In the next version of CLAAS we will apply a more extensive analysis concerning the influence of NWP fields on the cloud top products, since they are most sensitive to variations in temperature and humidity profiles.

We will further investigate the influence of viewing angles on cloud optical thickness and ice water path that led to the discontinuities in bias.

The Calypso and CloudSat datasets were found to deliver most valuable information for the analysis of CLAAS at Level 2 stage. In the future this allows us to analyze extremely high resolved features and helps for example in the assessment of cloud top pressure and NWP profiles.

6 Data format description

CLAAS products are provided as NetCDF (Network Common Data Format) files (http://www.unidata.ucar.edu/software/netcdf/). The data files are created following NetCDF Climate and Forecast (CF) Metadata Convention version 1.5 (http://cf-pcmdi.llnl.gov/) and NetCDF Attribute Convention for Dataset Discovery version 1.0.

For data processing and conversion to various graphical packages input format, CM SAF recommends the usage of the climate data operators (CDO), available under GNU Public License (GPL) from MPI-M (http://www.mpimet.mpg.de/~cdo).

6.1 Data format description of non-averaged products

Level 2 data are stored in hdf5-Format. Each hdf5 file has a predetermined structure and is composed of attributes, variables and nested structures. Since our non-averaged data products stem from two different software packages, the hdf5 file structure is not equal. A complete description of the data fields in the cloud mask, cloud type and cloud top products can be found in [RD 6]. The content of the cloud optical properties files is explained in the following.

6.1.1 Attributes

All data fields posses general attributes, which are listed and described in Table 6-1.

Table 6-1: Attributes of each variable such as COT in a non-averaged cloud optical properties hdf5 file.

Name	Description
description	Long name of the variable
gain	Scaling factor
intercept	Offset
no_data_value	The fill value for pixel without data

The absolute value of the respective variable y is composed of the value in the datafield x together with gain and intercept:

$$Y = \text{gain} * x + \text{intercept}$$

6.1.2 Data fields

The variables contained in one cloud microphysical properties file are listed and described in Table 6-2.

Table 6-2: Data fields contained in a non-averaged cloud optical properties file.

Name	Description
cot	Clod optical thickness
cph	Cloud phase
cph_ir	Cloud phase infrared only
cwp	Cloud water path
dcot	Error in COT
dcwp	Error in CWP
dreff	Error in effective radius
reff	Effective radius

6.1.3 General attributes

A cloud optical properties hdf5 file also possesses general attributes that are valid for all variables contained in this file, the attributes are described in Table 6-3

Table 6-3: General attributes of a non-averaged hdf5 cloud optical properties file.

Name	Description
version	Version of the Algorithm
sec_1970	Date in seconds from 1970
orbit_number	Not applicable for a geostationary sensor
description	Description of the file contents
satellite_id	Name of the satellite

Additionally the structure “Region” is included that describes the geolocation of the data fields, its attributes are described in Table 6-4.

Table 6-4: Contents of the structure “Region” in a non-averaged cloud optical properties hdf5 file.

Name	Description
area_extent	contains subsatellite point, area extent as well as xscaling and yscaling
id	Not set
name	Not set
pcs_id	Not set
pcs_Def	Not set

6.2 Monthly and daily mean data file contents

A common NetCDF file consists of dimensions, variables, and attributes. These components can be used together to capture the meaning of data and relations among data. All CLAAS products files are built following the same design principles. All files contain general variables, which are common for all files, and product specific variables. The latter are three-dimensional, except for the Joint Cloud property histograms. Dimension of all three-dimensional fields are named *time*, *lon*, *lat*. For the JCHs, additional two dimensions for COT and CTP bin are included. General variables of each file are *time*, *climatology_bounds*, *latitude*, and *longitude* (see section 6.2.1). All data fields, which are described in section 6.2.3, also contain specific attributes as given in section 6.2.2. Global attributes of each file are reported in section6.2.4.

6.2.1 General variables

time
start of averaging/composite time period
[days counted from 1970-01-01]

climatology_bounds
two-dimensional array defining the averaging/composite time period
(only used for monthly mean diurnal cycle products)

latitude
geographical latitude of grid-box centre [degree_north]

longitude
geographical longitude of grid-box centre [degree_east]

Note, the files containing the equal-area polar grid data provide two-dimensional *latitude* and *longitude* fields due to the deviation from regular grids.

6.2.2 Attributes

Table 6-5 summarizes the attributes which are assigned to each data field in the NetCDF files.

Table 6-5: Attributes assigned to variables in NetCDF.

Name	Description
long_name	long descriptive name
standard_name	standard name that references a description of a variable's content in the CF standard name table
units	physical unit [udunits standards]
valid_min	smallest valid value of a variable
valid_max	largest valid value of a variable
scale_factor	The data are to be multiplied by this factor after it is read.
add_offset	This number is to be added to the data after it is read. If scale_factor is present, the data are first scaled before the offset is added.
_FillValue	This number represent missing or undefined data. Missing values are to be filtered before scaling.
missing	same as _FillValue

Name	Description
cell_methods	method used to derive data that represents cell values

6.2.3 Product specific data fields

6.2.3.1 Fractional cloud coverage

cfc(time, lon, lat)
: field containing the mean cloud fractional coverage value given in percent, valid range is between 0 and 100;

cfc_nobs(time, lon, lat)
: field containing the number of observations used to create mean CFC

cfc_day(time, lon, lat)
: field containing the mean daytime cloud fractional coverage given in percent, valid range is between 0 and 100;

cfc_day_nobs(time, lon, lat)
: field containing the number of observations used to create mean daytime CFC

cfc_night(time, lon, lat)
: field containing the mean nighttime cloud fractional coverage given in percent, valid range is between 0 and 100;

cfc_night_nobs(time, lon, lat)
: field containing the number of observations used to create mean nighttime CFC

6.2.3.2 Cloud phase

cph(time, lon, lat)
: field containing the mean liquid cloud fraction given in percent, valid range is between 0 and 100;

cph_nobs(time, lon, lat)
: field containing the number of observations used to create mean CPH

6.2.3.3 Cloud top level

ctp_arith_mean(time, lon, lat)
: field containing the arithmetical mean cloud top pressure, valid range is between 0 and 1050 hPa

ctp_geometric_mean(time, lon, lat)
: field containing the geometrical (logarithmic) mean cloud top pressure, valid range is between 0 and 1050 hPa

ctp_arith_stdv(time, lon, lat)
: field containing the standard deviation over CTP values used to calculated arithmetical mean CTP

cth_arith_mean(time, lon, lat)
: field containing the arithmetical mean cloud top height, valid range is between 0 and 15000 meter

cth_arith_stdv(time, lon, lat)
: field containing the standard deviation over CTH values used to calculated arithmetical mean CTH

ctt_arith_mean(time, lon, lat)

field containing the arithmetical mean cloud top temperature, valid range is between 0 and 15000 meter

ctt_arith_stdv(time, lon, lat)
field containing the standard deviation over CTT values used to calculated arithmetical mean CTT

nobs(time, lon, lat)
field containing the number of observations used to create CTO

6.2.3.4 Cloud optical thickness

cot(time, lon, lat)
field containing the mean cloud optical thickness (COT), considering all clouds

cot_stdv(time, lon, lat)
field containing the COT standard deviation, considering all clouds

cot_err(time, lon, lat)
field containing the mean COT retrieval error, considering all clouds

cot_nobs(time, lon, lat)
field containing the number of observations, considering all clouds

cot_liq(time, lon, lat)
field containing the mean cloud optical thickness (COT), considering liquid clouds

cot_liq_stdv(time, lon, lat)
field containing the COT standard deviation, considering liquid clouds

cot_liq_err(time, lon, lat)
field containing the mean COT retrieval error, considering liquid clouds

cot_liq_nobs(time, lon, lat)
field containing the number of observations, considering liquid clouds

cot_ice(time, lon, lat)
field containing the mean cloud optical thickness (COT), considering ice clouds

cot_ice_stdv(time, lon, lat)
field containing the COT standard deviation, considering ice clouds

cot_ice_err(time, lon, lat)
field containing the mean COT retrieval error, considering ice clouds

cot_ice_nobs(time, lon, lat)
field containing the number of observations, considering ice clouds

6.2.3.5 Liquid water path

lwp(time, lon, lat)
field containing the mean liquid water path

stdv(time, lon, lat)
field containing the standard deviation over LWP values used to calculated mean LWP

nobs(time, lon, lat)
field containing the number of observations used to calculate mean IWP

6.2.3.6 Ice water path

iwp(time, lon, lat)
field containing the mean ice water path

stdv(time, lon, lat)
field containing the standard deviation over IWP values used to calculated mean IWP

nobs(time, lon, lat)

field containing the number of observations used to calculate mean IWP

6.2.3.7 Joint Cloud property Histograms

jch(time, lon, lat, ncot, nctp)

field containing the number of occurrences of specific combinations of COT and CTP ranges at given spatial location. In the notation above, *ncot* and *nctp* give the number of COT and CTP bins. The Joint Cloud property Histograms are defined on coarser spatial resolution (1.0°) compared to all other products (0.25°)

6.2.3.8 One-dimensional histograms

ctp1dhist(time,lon,lat,nctp),
cot1dhist(time,lon,lat,ncot),
iwp1dhist(time,lon,lat,niwp),
lwp1dhist(time,lon,lat,nlwp)

fields containing the number of occurrences of specific CTP, COT, IWP and LWP ranges at given spatial location. In the notation above, *nctp*, *ncot*, *niwp* and *nlwp* give the number of CTP, COT, IWP and LWP bins.

6.2.4 Global atttributes

Table 6-6 contains the global attributes of CLAAS final product files. Possible values of the attributes are also given as well as explanations.

Table 6-6: Overview of global attributes of NetCDF files of CLAAS cloud products and possible corresponding values.

Name	Description
title	CM SAF Cloud property dAtaset Using SEVIRI (CLAAS), edition 1
summary	This file contains MSG SEVIRI Climate Data Records (CDR) produced by the Satellite Application Facility on Climate Monitoring (CM SAF).
product_class	Cloud products, daily/monthly means/histograms/diurnal cycles
Conventions	conventions followed, "CF-1.5" for all files
Metadata_Convention	conventions followed, "Unidata Dataset Discovery v1.0" for all files
institution	EUMETSAT Satellite Application Facility on Climate Monitoring (CM SAF)
Digital_Object_Identifier	not assigned yet
creator_url	http://www.cmsaf.eu
creator_email	contact.cmsaf@dwd.de
references	http://www.cmsaf.eu
source	MSG SEVIRI Level 1B
cdm_data_type	grid
filename	*original filename* (case dependent)

Name	Description
time_coverage_start	*temporal coverage start of the data [ISO8601 date]* (case dependent)
time_coverage_end	*temporal coverage end of the data [ISO8601 date]* (case dependent)
time_coverage_duration	*temporal coverage duration of the data [ISO8601 duration]* (case dependent)
time_coverage_resolution	*temporal coverage resolution of the data [ISO8601 duration]* (case dependent)
geospatial_lat_units	*latitude attributes unit* (degree_north)
geospatial_lat_resolution	*latitude grid resolution* (0.05/0.25f)
geospatial_lat_min	*latitude bounding box minimum* (-90.f)
geospatial_lat_max	*latitude bounding box maximum* (90.f)
geospatial_lon_units	*longitude attributes unit* (degree_east)
geospatial_lon_resolution	*longitude grid resolution* (0.05/0.25f)
geospatial_lon_min	*longitude bounding box minimum* (-90.f)
geospatial_lon_max	*longitude bounding box maximum* (90.f)
dataset_version	*SEVIRI dataset version*
sev_major_version_number	*SEVIRI major release version*
sev_minor_version_number	*SEVIRI minor release version*
sev_parameter_name	*SEVIRI parameter name*
sev_parameter_id	*SEVIRI parameter ID*
processed_satellites	*satellites id's processed for this mean and corresponding orbits*
CM SAF_parameter_id	*CM SAF product identifier*
CM SAF_parameter_code	*CM SAF product name*
L3_processor	*L3 processor version used to create L3 products*
L2_processors	*L2 processor version used to create L2 products*
L1_intercalibration	*intercalibration version applied*
reference_documents	*Reference documents products*

7 Data ordering via the Web User Interface (WUI)

User services are provided through the CM SAF homepage www.cmsaf.eu. The user service includes information and documentation about the CM SAF and the CM SAF products, information on how to contact the user help desk and allows to search the product catalogue and to order products.

On the main webpage, a detailed description how to use the web interface for product search and ordering is given. We refer the user to this description since it is the central and most up to date documentation. However, some of the key features and services are briefly described in the following sections.

7.1 Product ordering process

You need to be registered and logged in to order products. A login is provided upon registration, all products are delivered free of charge. After the selection of the product, the desired way of data transfer can be chosen. This is either via a temporary ftp account (the default setting), or by CD/DVD or email. Each order will be confirmed via email, and the user will get another email once the data have been prepared. If the ftp data transfer was selected, this second email will provide the information on how to access the ftp server.

7.2 Contact User Help Desk staff

In case of questions the contact information of the User Help Desk (e-mail address contact.cmsaf@dwd.de, telephone and fax number) are available via the CM SAF main webpage (http://www.cmsaf.eu) or the main page of the Web User Interface.

7.3 Feedback/User Problem Report

Users of CM SAF products and services are encouraged to provide feedback on the CM SAF product and services to the CM SAF team. Users can either contact the User Help Desk (see chapter 7.2) or use the “User Problem Report” page. A link to the “User Problem Report” is available either from the CM SAF main page (www.cmsaf.eu) or the Web User Interface main page.

7.4 Service Messages / log of changes

Service messages and a log of changes are also accessible from the CM SAF main webpage (www.cmsaf.eu) and provide useful information on product status, versioning and known deficiencies.

8 Copyright and Disclaimer

The user of CM SAF data agrees to respect the following regulations:

Copyright

Acknowledgement and Identification

When exploiting EUMETSAT/CM SAF data you are kindly requested to acknowledge this contribution accordingly and make reference to the CM SAF, e.g. by stating "The work performed was done (i.a.) by using data from EUMETSAT's Satellite Application Facility on Climate Monitoring (CM SAF)". It is highly recommended to clearly identify the product version used. An effective way to do this is the citation of CM SAF data records via the digital object identifier (doi). The doi of the data sets can be retrieved through (http://www.cmsaf.eu/DOI).

Re-distribution of CM SAF data

Please do not re-distribute CM SAF data to 3rd parties. The use of the CM SAF products is granted free of charge to every interested user, but we have an essential interest to know how many and what users the CM SAF has. This helps to ensure of the CM SAF operational services as well as its evolution according to users needs and requirements. Each new user shall register at CM SAF in order to retrieve the data.

Feedback

We are keen to learn of what use the CM SAF data are. So please feedback your experiences and your application area of the CM SAF data. EUMETSAT CM SAF is user driven service and is committed to consider the needs and requirements of its users in the planning for product improvements and additions. Users are invited to provide their specific requirements on future products for their applications.

9 References

Baum, B.A., P.F. Soulen, K.I. Strabala, M.D. King, S.A. Ackerman, W.P. Menzel, and P. Yang, 2000: Remote sensing of cloud properties using MODIS airborne simulator imagery during SUCCESS 2. Cloud thermodynamic phase, *J. Geophys. Res.*, **105**, 11781 – 11792, doi: 10.1029/1999JD901090.

Berk, A., G. P. Anderson, P. K. Acharya, J. H. Chetwynd, L.S. Bernstein, E. P. Shettle, M. W. Matthew, and S. M. Adler-Golden, 2000: MODTRAN4 Version 2 Users Manual. Technical report, Air Force Materiel Command, Air Force Research Laboratory, Space Vehicles Directorate, Hanscom AFB, MA 01731, USA.

Carbajal Henken, C.K., M.J. Schmeits, H. M. Deneke and R.A. Roebeling, 2011: Using MSG-SEVIRI cloud physical properties and weather radar observations for the detection of Cb/TCu clouds, J. *Appl. Meteor. Climatol*., **50**, 1587–1600, doi: 10.1175/2011JAMC2601.1

Dee et al. (35 named authors), 2011: The ERA-Interim reanalysis: configuration and performance of the data assimilation system, Quart. J. Royal Met. Soc., **137** (656), 553 - 597. Online version: http://onlinelibrary.wiley.com/doi/10.1002/qj.828/abstract.

De Haan, J. F., P. Bosma, and J. W. Hovenier, 1987: The adding method for multiple scattering calculations of polarized light, *Astron. Astrophys*., **183**, 371-391.

Derrien, M. and H. Le Gléau, 2005, MSG/SEVIRI cloud mask and type from SAFNWC, International Journal of Remote Sensing, **26**, No. 21, 4707–4732.

Derrien, M. and H.Le Gléau, 2010: Improvement of cloud detection near sunrise and sunset by temporal differencing and region-growing techniques with real-time SEVIRI, International Journal of Remote Sensing, **31**, No. 7, 1765-1780.

Fuchs, P., 2012: Satellite Application Facility on Climate Monitoring Evaluation Report Change of NWP Input – SEVIRI, SAF/CM/DWD/ER/SEVIRI/1.

Goyens, C., D. Lauwaet, M. Schröder, M. Demuzere, N. van Lipzig, 2011: Tracking Mesoscale Convective Systems in the Sahel: relation between cloud parameters and precipitation, *Int. J. Clim*., doi: 10.1002/joc.2407.

Haywood, J.M., S.R. Osborne, S.J. Abel, 2004: The effect of overlying absorbing aerosol layers on remote sensing retrievals of cloud effective radius and cloud optical depth, *Quart. J. Roy. Meteorol. Soc*., **130**, 779-800, doi: 10.1256/qj.03.100.

Hess, H., R. B. A. Koelemeijer, and P. Stammes, 1998: Scattering matrices of imperfect hexagonal crystals. *J. Quant. Spectrosc. Ra*., **60**, 301–308.

Knap, W. H., L. C. Labonnote, G. Brogniez, and P. Stammes, 2005: Modeling total and polarized reflectances of ice clouds: evaluation by means of POLDER and ATSR-2 measurements. *Appl. Optics*, **44**, 4060-4073.

Kniffka, A., M. Lockhoff, R. Hollmann, 2010: Latitudinal variation of Cloud Top Height throughout the seasons as seen from SEVIRI, AIRS and ATSR-2, *Geophysical Research Abstracts*, **12**, EGU2010-13095, 2010, EGU General Assembly 2010.

Meirink, J.F., R.A. Roebeling and P. Stammes, 2009: Atmospheric correction for the KNMI Cloud Physical Properties retrieval algorithm, KNMI publication: TR-304, 17/2/2009, pp22.

Minnis, P., K. N. Liou, and Y. Takano, 1993: Inference of Cirrus Cloud Properties Using Satellite-observed Visible and Infrared Radiances. Part I: Parameterization of Radiance Fields. *J. Atmos. Sci.*, **50**, 1279–1304.

Nakajima, T., and M. D. King, 1990: Determination of the Optical Thickness and Effective Particle Radius of Clouds from Reflected Solar Radiation Measurements. Part 1: Theory. *J. Atmos. Sci* ., **47**, 1878-1893.

Platnick, S., 2001: A superposition technique for deriving mean photon scattering statistics in plane-parallel cloudy atmospheres, *J. Quant. Spectrosc. Radiat. Transfer*, **68**, 57-73.

Roebeling, R. A., A. J. Feijt, and P. Stammes, 2006: Cloud property retrievals for climate monitoring: implications of differences between SEVIRI on METEOSAT-8 and AVHRR on NOAA-17, *J. Geophys. Res*., **111**, D20210, doi:10.1029/2005JD006990.

Roebeling, R. A., H. M. Deneke and A. J. Feijt, 2008: Validation of cloud liquid water path retrievals from SEVIRI using one year of CloudNET observations, *J. Appl. Meteorol. Clim*., **47**, 206-222.

Roebeling, R. A., and E. van Meijgaard, 2009: Evaluation of the Daylight Cycle of Model-Predicted Cloud Amount and Condensed Water Path over Europe with Observations from MSG SEVIRI, *J. Clim*., **22** (7), 1749-1766 DOI: 10.1175/2008JCLI2391.1.

Siewert, C. W., M. Koenig and J. R. Mecikalski, 2010: Application of Meteosat second generation data towards improving the nowcasting of convective initiation, *Meteorol. Appl*., **17**, 4, *DOI 10.1002.*

Stammes, P., 2001: Spectral radiance modeling in the UV-Visible range. IRS 2000: Current problems in Atmospheric Radiation, edited by W.L. Smith and Y.M. Timofeyev, pp 385-388, A. Deepak Publ., Hampton, VA.

Stephens, G. L., 1978: Radiation profiles in extended water clouds: II. Parameterization schemes. *J. Atmos. Sci*., **35**, 2123-2132.

Trolez, M, K.-G. Karlsson, S. Johnston and P. Albert, 2008: The impact of varying NWP background information on CM-SAF cloud products, CM SAF Visiting Scientist Report, *SMHI Reports Meteorology*, **128**, 41 pp.

Wolters, E. L .A., H. M. Deneke, B. J. J. M. van den Hurk, J. F. Meirink, and R. A. Roebeling, 2010: Broken and inhomogeneous cloud impact on satellite cloud particle effective radius and cloud-phase retrievals, *J. Geophys. Res*., **115**, doi:10.1029/2009JD012205.

Wolters, E. L. A., R.A. Roebeling, and A. J. Feijt, 2008: Evaluation of cloud-phase retrieval methods for SEVIRI onboard Meteosat-8 using ground-based lidar and cloud radar data, *J. Appl. Meteorol. Clim*., **47**, 1723-1738, doi:10.1175/2007JAMC1591.1.

10 Glossary

ATBD	Algorithm Theoretical Baseline Document
AVHRR	Advanced Very High Resolution Radiometer
CALIPSO	Cloud-Aerosol Lidar and Infrared Pathfinder Satellite Observations
CALIOP	Cloud-Aerosol Lidar with Orthogonal Polarisation
CDO	Climate Data Operators
CDOP	Continuous Development and Operations Phase
CFC	Fractional Cloud Cover
CLAAS	CM SAF CLoud property dAtaset Using SEVIRI
CM SAF	Satellite Application Facility on Climate Monitoring
COT	Cloud Optical Thickness
CPH	Cloud Phase
CPR	Cloud Profiling Radar
CTH	Cloud Top Height
CTO	Cloud Top product
CTP	Cloud Top Pressure
CTT	Cloud Top Temperature
CPP	Cloud Physical Properties
DRI	Delivery Readiness Inspection
DWD	Deutscher Wetterdienst (German MetService)
ECMWF	European Centre for Medium Range Forecast
ECV	Essential Climate Variable
ERA-Interim	Second ECMWF Re-Analysis dataset
EUMETSAT	European Organisation for the Exploitation of Meteorological Satellites
FCDR	Fundamental Climate Data Record
GCOS	Global Climate Observing System
IWP	Ice Water Path
JCH	Joint Cloud properties Histogram
MODIS	Moderate Resolution Imaging Spectroradiometer
MSG	Meteosat Second Generation
KNMI	Koninklijk Nederlands Meteorologisch Institut
LWP	Liquid Water Path
NetCDF	Network Common Data Format
NOAA	National Oceanic & Atmospheric Administration
NWC SAF	SAF on Nowcasting and Very Short Range Forecasting
NWP	Numerical Weather Prediction
PRD	Product Requirement Document
PUM	Product User Manual
SEVIRI	Spinning Enhanced Visible and InfraRed Imager
SAF	Satellite Application Facility
SMHI	Swedish Meteorological and Hydrological Institute

SYNOP	Synoptic observations
TCDR	Thematic Climate Data Record

11 Summary table of validation results regarding product accuracy

Table 11-1 shows the achieved accuracies of the cloud products as discussed in [RD 1]. The acronyms used are: SYNOP = Synoptical surface observations, CALIPSO = Cloud-Aerosol Lidar and Infrared Pathfinder Satellite Observation, MODIS=Moderate Resolution Imaging Spectroradiometer. All references are described in detail in [RD 1].

Table 11-1: Summary table of validation results as given in [RD 1]. For CFC and CPH (being defined as percentage values), results are given as absolute values (not relative). In contrast, results for LWP and IWP are given as relative errors.

Product		Accuracy requirement (Mean error or Bias))	Achieved accuracies
Cloud Fractional Cover	(CFC)	10% (MM, abs.) 15% (DM)	2.7 % (SYNOP) 8.7 % (MODIS)
Cloud Top Height	(CTH)	800 m	-646.92 m, -10.7 % (MM) -872 m, -14.4 % (DM) (Cloudnet) -687.2 m, -11.6 % (CALIOP) -83.2 m, -1.3 % (CPR)
Cloud Top Pressure	(CTP)	45 hPa	-160 hPa (MODIS)
Cloud Optical Thickness	(COT)	10%	-9.9 % (MODIS)
Cloud Phase	(CPH)	0.05	-0.03 (MODIS-IR) 0.14 (MODIS-OPT)
Liquid Water Path	(LWP)	10%	-0.3 % (MODIS) 0.1 -1.7 % (MICROWAVE)
Ice Water Path	(IWP)	20%	-6.2 % (MODIS)
Joint Cloud Histogram	(JCH)	n/a	n/a

-